Strain Stiffening in Synthetic and Biopolymer Networks

Kendra A. Erk, Kevin J. Henderson, and Kenneth R. Shull*

Department of Materials Science and Engineering, Northwestern University, Evanston, Illinois 60208

Received February 3, 2010; Revised Manuscript Received March 13, 2010

Strain-stiffening behavior common to biopolymer networks is difficult to reproduce in synthetic networks. Physically associating synthetic polymer networks can be an exception to this rule and can demonstrate strain-stiffening behavior at relatively low values of strain. Here, the stiffening behavior of model elastic networks of physically associating triblock copolymers is characterized by shear rheometry. Experiments demonstrate a clear correlation between network structure and strain-stiffening behavior. Stiffening is accurately captured by a constitutive model with a single fitting parameter related to the midblock length. The same model is also effective for describing the stiffening of actin, collagen, and other biopolymer networks. Our synthetic polymer networks could be useful model systems for biological materials due to (1) the observed similarity in strain-stiffening behavior, which can be quantified and related to network structure, and (2) the tunable structure of the physically associating network, which can be manipulated to yield a desired response.

Introduction

Many soft biological materials become stiffer when deformed.[1] Such nonlinear elastic behavior is referred to as strain stiffening and is defined as an increase in a material's elastic modulus with applied strain. Structural biopolymer networks display significant strain stiffening when deformed, such as the fibrin gels responsible for blood clotting[2] and actin filaments in cellular cytoskeletons.[3,4] These examples suggest a physiological relevance of the stiffening mechanism as a means to preventing damage from exposure to large deformations.[1] Therefore, understanding the strain-stiffening response is of primary importance when designing artificial biomaterials for structural applications such as tissue scaffolds. However, the synthetic reproduction of the stiffening response of biological materials remains elusive, complicating biomaterial design for structural applications. Most simple synthetic gels and rubbers deform linearly to large strains (e.g., polyacrylamide[5]) or exhibit a decrease in stiffness (e.g., natural rubber[6]) at intermediate strains. However, physically associating polymer networks are one class of synthetic networks that often undergo strain stiffening at relatively low values of strain without prior softening behavior.[7−9] Additionally, physically associating polymer networks are found to display exponential strain-stiffening behavior that is strikingly similar to the stiffening behavior of biopolymer materials. The strain-stiffening behavior of a variety of biopolymer networks from the data collected by Storm and co-workers[1] is illustrated in Figure 1. A striking feature of these data is that they can all be represented by the following simple form, represented by the solid lines in Figure 1:

$$\tau = G_0\gamma \exp((\gamma/\gamma^*)^2) \qquad (1)$$

In this work, we show that eq 1 emerges from a strain energy function that can also be used to describe a series of physically associating, synthetic polymer gels. In addition, we show that the parameters G_0 and γ^* can be directly related to molecular features of these synthetic analogs.

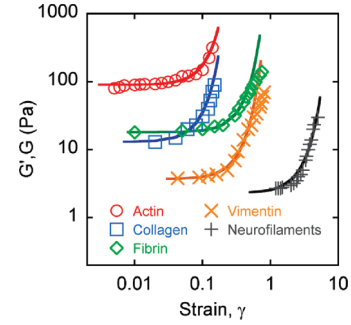

Figure 1. Data taken from Storm et al.[1] Strain stiffening of common biopolymer networks. G' measured at 10 rad/s for actin, fibrin, collagen, and vimentin. G is obtained from steady shear experiments for the neurofilaments. Solid lines represent eq 1 of the exponential strain energy function for each network, using values for G_0 and γ^* shown in Table 3.

In general, physically associating networks are self-assembled polymer networks composed of macromolecules in solution interconnected by physical cross-links. The physical cross-links consist of weak, noncovalent bonds formed by a variety of intermolecular interactions such as Coulombic attractions,[10] hydrogen bonding,[11] and enthalpic associations.[12] Some physically associating systems have cross-link bonding energies on the order of the thermal energy, k_bT, such that bond formation is completely reversible. In these cases, the bonds have lifetimes that can be strongly dependent on the temperature.[13,14] In appropriately designed materials, including the triblock copolymer solutions investigated herein, the physical cross-links are created and annihilated rapidly at elevated temperatures, resulting in the formation of a viscous liquid. The bond lifetimes increase dramatically as the temperature is reduced, such that at low temperatures these solutions behave as elastic materials. A variety of aqueous-based systems also exist where this behavior is reversed, with the more elastic state existing at higher temperatures.[15−17] Thermoreversible systems are important in a variety of material processing applications,[18,19] are useful as stimuli-responsive materials,[20,21] and have numerous biomedical applications.[22−25]

* To whom correspondence should be addressed. E-mail: k-shull@northwestern.edu.

10.1021/bm100136y
Published on Web 04/14/2010

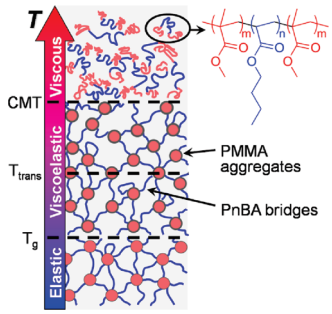

Figure 2. Schematic representation of thermoreversible behavior with increasing temperature of a model, physically associating network of symmetric triblock copolymers in a midblock-selective solvent. Adapted from *Macromolecules* **2003**, *36* (6), p 2001.

The primary physically associating network investigated here is a model network composed of symmetric triblock copolymer molecules dissolved in 2-ethyl-1-hexanol. The triblock copolymer molecules are linear polymer chains containing two poly(methyl methacrylate) (PMMA) end blocks separated by a poly(*n*-butyl acrylate) (PnBA) midblock (see Figure 2). These molecules are synthesized by anionic polymerization, allowing precise control over the molecular weight of each block while maintaining low polydispersity.[26] The following is an overview of the self-assembled structure, the dominant enthalpic interactions, and the linear mechanical properties of the network, as characterized in previous work (for details, refer to Drzal et al.[12] and Seitz et al.[27]).

Self-assembly of the network is driven by the temperature dependence of the enthalpic interaction parameter between the solvent and the end blocks.[12] For the PMMA/alcohol system, this temperature dependence is unusually strong within the experimentally accessible temperature window, resulting in the temperature-dependent network formation shown schematically in Figure 2. At high temperatures (>80 °C), the triblock copolymer is fully dissolved in the solvent, forming a free-flowing, low-viscosity liquid. Below the critical micelle temperature (CMT; i.e., order−disorder transition), the PMMA end blocks self-assemble into spherical aggregates to minimize their interaction with the solvent. The aggregates act as physical cross-links, interconnected by flexible PnBA midblocks, and this network structure results in the formation of a viscoelastic liquid. As the system is cooled below the glass transition temperature (T_g) of the partially solvated PMMA end blocks, the physical structure of the network remains unchanged. However, the exchange rate of the end blocks between neighboring aggregates diminishes, and a strong, elastic-like network is formed with a well-defined molecular structure.[27] These networks are actually viscoelastic materials with a relaxation time that is highly temperature dependent. We define the transition temperature (T_{trans}) between liquid-like and solid-like mechanical behavior as the temperature at which the relaxation time is 0.1 s, as measured by oscillatory shear rheometry.[27] This transition temperature is dependent on the structure and concentration of the triblock copolymer in the network and ranges from 30−60 °C for the materials investigated herein (see Table 1).

In this study, the strain-stiffening response of the network is primarily characterized at $T \ll T_{trans}$, where the relaxation times are very long (>10^5 s).[27] In this elastic regime, the linear elastic properties of the network are described by the modulus, which is determined by the concentration of elastically active, PnBA midblock "bridges" that span different PMMA end block aggregates. The fraction of bridging chains in a network (as well as the number of chains) increases with polymer concentration, leading to stiffer networks at higher concentrations.[27,28] For the networks investigated here, polymer volume fractions were limited to ≤0.10, dictated by the torque limit of the rheometer employed to measure the properties of these networks. The chosen concentrations were slightly greater than the critical concentrations corresponding to the percolation threshold at which the bridging midblocks form a fully elastic network.[29]

Table 1. Compositions of Physically Associating Networks[a]

triblock copolymer	A, PMMA M_w (g/mol)	B, PnBA M_w (g/mol)	C, PMAA M_w (g/mol)	Φ_p	T_{trans} (°C)
$A_9B_{53}A_9$	8900	53000		0.050	34
$A_{23}B_{31}A_{23}$	23000	31000		0.070	58
$A_{25}B_{116}A_{25}$	25000	116000		0.035	56
$A_{22}C_{45}A_{22}$	22000		45000	0.10	
$A_{34}C_{114}A_{34}$	34000		114000	0.10	

[a] Subscripts denote the block molecular weight in kg/mol for A = poly(methyl methacrylate), B = poly(*n*-butyl acrylate), and C = poly(methacrylic acid).

The goal of the present work is to characterize the nonlinear stress response of these model elastic network. Experiments demonstrate a clear correlation between midblock length and strain stiffening. To demonstrate the generality of the observed nonlinear response to hydrogels that are of more obvious biological relevance, we also describe the stiffening behavior of a physically associating (but nonthermally reversible) water-based network. Stiffening is quantified using an exponential strain energy function with a single fitting parameter related to the midblock length. This constitutive model gives rise to the same functional form of the strain-stiffening behavior that is observed for the biological networks (Figure 1). This similarity indicates that our synthetic polymer networks are useful model systems for studying the mechanical response of a range of biological materials.

Experimental Methods

Materials. Poly(methyl methacrylate)-poly(*n*-butyl acrylate)-poly(methyl methacrylate) triblock copolymers of various molecular weights and block fractions were provided by Kuraray, Co. (Japan) and were used as received. To form the physically associating networks, triblock copolymer was dissolved in 2-ethyl-1-hexanol (Sigma Aldrich Co.; used as received) at temperatures above 80 °C in a magnetically stirred, sealed vial. Hydrogels were formed from poly(methyl methacrylate)-poly(methacrylic acid)-poly(methyl methacrylate) copolymers according to procedures described below. The characteristics of these polymers and the overall polymer volume fractions in the networks (Φ_p) are listed in Table 1.

Methods. A stress-controlled Anton-Paar Physica MCR 300 rheometer (Ashland, VA) with Peltier temperature control was employed for all shear deformation experiments. For thermoreversible networks, samples were contained in a Couette fixture (single-gap, 1.1 mm) with a fixture cover to prevent solvent loss. Samples were loaded in a fluid state, allowed to equilibrate for 5 min, and subsequently cooled and equilibrated at the temperature of interest. The thermoreversibility of the network and the fast equilibration time allowed for multiple shear deformation experiments to be performed sequentially on a single sample. After each experiment, the sample was heated to $T \gg T_{trans}$ and allowed to rest in a low-viscosity fluid state for at least 5 min. After cooling and equilibrating at the temperature of interest, a new experiment was performed. Experimental results were found to be entirely reproducible and in agreement for one sample deformed multiple times and for different samples with the same compositions. Unless otherwise noted, the networks were investigated at least 25 °C below T_{trans}, such that the characteristic relaxation time of the network was greater than 10^5 s and the network behaved as an elastic material.[27]

Hydrogel Formation and Testing. As a proof-of-concept experiment, elastic triblock copolymer hydrogels were created by solvent exchange and deformed by shear rheometry. The solvent exchange process and resulting structure of the network are described in detail elsewhere.[30] Poly(methyl methacrylate)-poly(methacrylic acid)-poly(methyl methacrylate) triblock copolymer was synthesized and dissolved in dimethyl sulfoxide (DMSO) at a polymer volume fraction of 0.10. Two triblock copolymers were investigated: a short-midblock polymer ($A_{22}C_{45}A_{22}$ from Table 1) and a long-midblock polymer ($A_{34}C_{114}A_{34}$ from Table 1). As the DMSO solvent is replaced with water, the polymers self-assemble into an elastic network structure, with hydrophobic PMMA end block aggregates interconnected by hydrophilic PMAA midblocks. Solvent exchange with water was performed while the DMSO−polymer solution was contained in a parallel-plate rheometer fixture (1.0 mm gap, 12.5 mm radius; Anton-Paar Physica MCR 300 rheometer) in order to ensure strong adhesion between sample and fixture. Experiments were performed at room temperature. The samples were allotted 2 h to equilibrate with water surrounding the fixture, sufficient time for the outer portions of the samples to form elastic hydrogels ($G' \gg G''$) at room temperature. The time for full completion of the solvent-exchange process is on the order of 140 h (assuming a collective diffusion coefficient of $D_c \approx 8 \times 10^{-7}$ cm^2 s^{-1} and diffusion distance equal to the fixture radius of 12.5 mm).[30] For the solvent-exchange times used in our experiments, only the outer portion of the sample had gelled, and thus, we were unable to quantitatively determine the elastic modulus of these samples. The strain-stiffening behavior of the hydrogels can still be quantified by this approach, however.

Strain-Stiffening Model. To quantify the underlying physics of the strain-stiffening behavior and make connections with the structure of the physically associating networks, deformation-dependent strain energy functions can be used to predict nonlinear elasticity. In this study, the following expression is used to describe the strain energy density, U,

$$U = \frac{G_0}{2} J^* \left[\exp\left(\frac{J_1}{J^*}\right) - 1 \right]; \quad J_1 = \lambda_1^2 + \lambda_2^2 + \lambda_3^2 - 3 \qquad (2)$$

where G_0 is the small-strain shear modulus and λ_1, λ_2, and λ_3 are the principal extension ratios. The quantity J_1 is closely related to the first strain invariant, I_1, commonly used in descriptions of large-strain elasticity ($J_1 = I_1 - 3$). The only fitting parameter here is J^*, which can be viewed as the characteristic value of J_1 above which strain-stiffening effects dominate the network behavior. At small strains, the model reduces to the Neo-Hookean model. This function was used previously to describe the large strain behavior of elastic, self-assembled triblock copolymer gels deformed in uniaxial compression experiments.[9] Additionally, an equivalent strain energy function has been applied to biological systems by Fung and co-workers[31] and was employed recently to describe the elasticity of stiff polymer networks.[32]

Assuming an incompressible material ($\lambda_1^2\lambda_2^2\lambda_3^2 = 1$) undergoing shear deformation in the 1−2 plane ($\lambda_3 = 1$, $\lambda_1 = \lambda_2^{-1}$), eq 2 can be modified to obtain a strain energy function in terms of shear strain, γ:

$$U_{\text{shear}} = \frac{G_0}{2} J^* \left[\exp\left(\frac{J_1}{J^*}\right) - 1 \right]; \quad J_1 = (\lambda_1 - \lambda_2)^2 = \gamma^2 \qquad (3)$$

By differentiating U_{shear} with respect to γ, we obtain the following expression for shear stress, τ:

$$\tau = G_0 \gamma \exp\left(\frac{\gamma^2}{J^*}\right) \qquad (4)$$

which is equivalent to eq 1, with $\gamma^* = \sqrt{J^*}$, the critical value of strain at which stiffening becomes dominant. This response function accounts for both the linear (G_0) and nonlinear (J^*) contributions to the overall stress response of the deformed material.

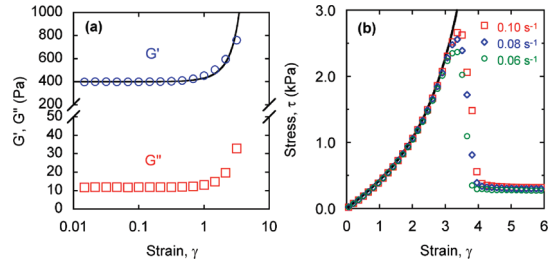

Figure 3. Linear and nonlinear deformation of a 5 v % $A_9B_{53}A_9$ physically associating network by shear rheometry at 10 °C (elastic regime, $T \ll T_{\text{trans}}$). (a) Storage (G') and loss (G'') moduli at $\omega = 10$ s^{-1} for a range of strain amplitudes. (b) Stress as a function of strain for steady shear deformation at rates of 0.06−0.10 s^{-1} (Wi $\gg$ 1). Solid lines are eq 4 from the exponential strain energy function for $G_0 =$ 400 Pa and $J^* = 14$.

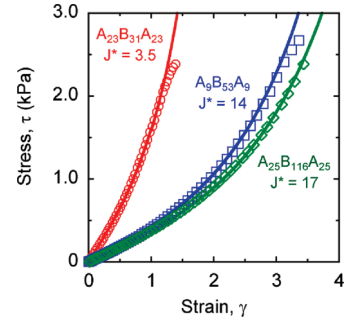

Figure 4. Strain-stiffening behavior for three physically associating networks ($A_{23}B_{31}A_{23}$, $G_0 = 1200$ Pa; $A_9B_{53}A_9$, $G_0 = 400$ Pa; $A_{25}B_{116}A_{25}$, $G_0 = 350$ Pa) during steady shear deformation at rates of 0.02, 0.1, and 0.1 s^{-1} (Wi $\gg$ 1). Solid lines correspond to eq 4, using the indicated values of J^*. Data beyond the stress maximum are omitted for clarity.

Results

The basic mechanical response of the physically associating networks in the elastic regime ($T << T_{\text{trans}}$) is shown in Figure 3 for the $A_9B_{53}A_9$ network. The dynamic oscillatory response (Figure 3a) displays clear strain stiffening for $\gamma \geq 0.3$. Strain stiffening is also observed in the steady shear response of the network for three relatively fast shear rates such that the Weissenberg numbers (Wi, defined here as the product of the relaxation time and the steady shear rate or radial frequency) are much greater than unity (Figure 3b). In this plot, stiffening of the network causes the stress to grow more than linearly with deformation, resulting in an upturn of the stress−strain curve at intermediate strains. As expected for elastic materials, the stress response to steady shearing is independent of the deformation rate at low and intermediate values of strain. At shear strains of ~3, a stress maximum is observed. This extreme nonlinearity is believed to be the result of a fracture-like instability in the system, reminiscent of fluid fracture,[33] and will be the focus of a future publication.

To investigate the relationship between network structure and strain stiffening, three physically associating networks composed of triblock copolymers with different midblock lengths (refer to Table 1) were deformed in steady shear at Wi $\gg$ 1, with the results displayed in Figure 4. The stress response at small strains is described by the small-strain shear modulus of the networks, G_0, which is a function of polymer concentration and structure.[27] At intermediate strains, strain stiffening is observed for all three networks, as shown in Figure 4. From this comparison we see that, as the length of the midblock increases, the critical shear strain at which stiffening dominates is suppressed toward larger

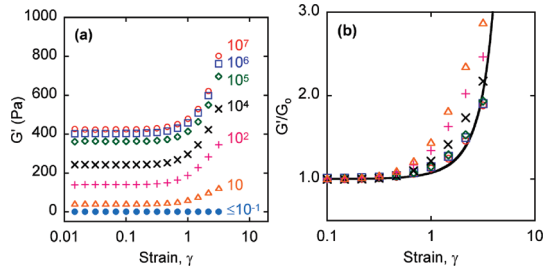

Figure 5. Storage modulus (a) and normalized modulus (b) for a 5 v % $A_9B_{53}A_9$ physically associating network undergoing oscillatory shear at $\omega = 10$ rad/s over a range of Wi. The solid line in (b) corresponds to eq 4 with $J^* = 14$.

values of strain, an effect clearly demonstrated by a comparison of networks with similar behavior in the linear regime ($A_9B_{53}A_9$ and $A_{25}B_{116}A_{25}$). The stress−strain relationship (eq 4) emerging from the exponential strain energy function as applied to the three networks (solid lines in Figure 4) gives a J^* value of 3.5 for $A_{23}B_{31}A_{23}$ and 17 for $A_{25}B_{116}A_{25}$. These values are equivalent to J^* values determined previously for uniaxial compression experiments of higher concentration $A_{23}B_{31}A_{23}$ and $A_{25}B_{116}A_{25}$ networks (note: $A_9B_{53}A_9$ was not tested in compression).[9] As indicated by Figure 4, values of J^* increase with midblock length.

Because our strain-stiffening model is an elastic model based on a strain energy function, it is expected to be valid only for large values of Wi, where the relaxation time of the network is long in comparison to the time scale of the experiment. To probe the limits of this approach for increasingly viscoelastic systems, a series of experiments was performed at different values of Wi. Our thermoreversible networks are exceptionally well suited for these investigations because Wi can be adjusted over a very broad range simply by adjusting the temperature (5−35 °C here, corresponding to a relaxation time scale of 10^6−10^{-2} s). In these networks the relaxation times increase by approximately an order of magnitude for each 5 °C decrease in temperature.[27] Results for different values of Wi from oscillatory shear experiments are shown in Figure 5. Figure 5a shows that the small-strain modulus (G_0) decreases substantially as Wi decreases, but that the onset of nonlinearity for the larger values of Wi occurs at a similar value of strain. This point is emphasized in Figure 5b, which shows the relative increase in the modulus as a function of strain amplitude for each of the values of Wi ≥ 10 from Figure 5a. A universal behavior consistent with eq 4 is observed for values of Wi ≥ 10^5 (corresponding to $T \leq 15$ °C), but a more complicated behavior is observed for the lower values of Wi. These lower values, indicative of more liquid-like behavior, require a more complicated analysis than is possible by a simple elastic model based on the strain energy. The fundamental results in this paper are most applicable to values of Wi that are substantially greater than unity.

Acrylic triblock copolymer hydrogels were created via solvent exchange to illustrate the existence of strain-stiffening behavior in model physically associating networks in a more biologically relevant solvent. As seen in Figure 6, the hydrogels strain-stiffen when deformed in shear. In the stiffening regime, the stress increases in an exponential fashion as described by eq 4, similar to the alcohol-based networks. Consistent with previous results, the onset of significant strain stiffening occurs at a larger value of strain for the hydrogel containing the long-midblock triblock copolymer ($A_{34}C_{114}A_{34}$) compared to the hydrogel containing the short-midblock triblock copolymer ($A_{22}C_{45}A_{22}$).

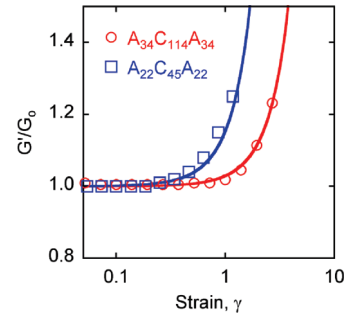

Figure 6. Normalized shear modulus for hydrogel samples during oscillatory shear at $\omega = 10$ s^{-1} as a function of the strain amplitude. Solid lines correspond to eq 4, with $G_0 = 13.1$ kPa and $J^* = 7$ for $A_{22}C_{45}A_{22}$ and $G_0 = 2.2$ kPa and $J^* = 35$ for $A_{34}C_{114}A_{34}$.

Discussion

The underlying structure of physically associating triblock copolymer networks, rubbery midblocks spanning end block aggregates, ultimately controls the mechanical response of the network to an applied stress. In general, when a transient polymer network is deformed, stress relaxation occurs by physical cross-link yielding and subsequent viscoplastic chain pull-out of the end blocks from their respective aggregates.[34] At the temperatures investigated here ($T << T_{trans}$), the end block segments are "frozen" or kinetically trapped in the glassy aggregates,[28] preventing chain pull-out at small-to-intermediate values of stress and forming a strain-stiffening, elastic network with extremely long relaxation times.

Elastic networks, even those with permanent network junctions and entanglements (e.g., natural rubber[6]), often exhibit strain-softening behavior. This behavior is attributed to the redistribution of internal stress due to progressive slip of entanglement points.[35] Strain softening was not observed for the physically associating networks investigated here, most likely because the molecular weights of the midblock strands were below the predicted entanglement threshold for these solvent-swollen materials.[27,36,37] In fact, these triblock copolymer networks were recently cited as excellent systems for strain-stiffening investigations due to their lack of entanglements.[38]

The strain-stiffening response of physically associating networks can be attributed to nonlinear stretching and finite extensibility of the network strands connecting neighboring network junctions.[7,9,38,39] In more viscous physically associating solutions, alternative explanations for strain stiffening and the related phenomenon of shear thickening have been presented,[8] such as deformation-induced increases in the number of elastically active strands or network components.[40,41] Based on the characterized structure of our triblock copolymer networks[27] and the stress responses observed here, we believe our physically associating networks evolve in the following manner during deformation: as the external shear stress is applied to the network, the distance between the end block aggregates increases with deformation and the rubbery midblock strands are stretched, adopting non-Gaussian conformations and causing a stiffening of the network. As the midblock is stretched to its maximum extensibility, the stiffening response becomes dominant, causing the stress to rapidly increase. Therefore, the critical value of strain at which stress-divergence occurs is expected to be controlled by the finite extensibility of the midblock.

This critical value of strain at which stiffening becomes dominant can be predicted from the following estimation for the maximum uniaxial extension ratio, λ_{max}, of a linear polymer chain

$$\lambda_{max} = \frac{l_{max}}{l_0} = \frac{nl \sin\left(\frac{\theta}{2}\right)}{l_0} \quad (5)$$

where l_{max} is the length of a fully extended polymer chain and l_0 is the end-to-end length of the unstretched polymer chain. The extended length can be estimated by assuming a *trans*-conformation of a polymer chain composed of n number of bonds of length l in the chain and an angle of θ between neighboring bonds.[42] For hydrocarbon polymer chains, a carbon−carbon single bond is approximately 0.154 nm in length with $\theta \sim 112°$. For the physically associating triblock copolymer networks investigated previously by Seitz et al.,[9] l_0 was determined from small-angle X-ray scattering results for undeformed triblock copolymer networks.[27] Scattering intensity patterns were fit with a Percus−Yevick hard-sphere model[43] in which the scattering core radius r_0 (∼radius of an end block aggregate) was obtained and the average center-to-center distance between aggregates, D, was calculated to estimate the unstretched midblock length, $l_0 = D - 2r_0$.

For the physically associating triblock copolymer networks investigated here, eq 5 was used to predict of the maximum extensibility ratio, λ_{max}, of the midblock strand in each network (see Table 2). To calculate l_0, values of D were extrapolated from previous X-ray scattering results of 10−30 v % triblock copolymer networks[27] and r_0 was assumed to be 5 nm, a reasonable approximation indicated by past work. The maximum extensibility ratio was converted to a maximum shear strain, γ_{max}, by the following equation:

$$\gamma_{max} = \lambda_{max} - \lambda_{max}^{-1} \quad (6)$$

As seen in Table 2, the predicted value of γ_{max} for the alcohol-based ABA networks is similar to the observed critical strain γ^*, which was calculated for each network from the fitting parameter, J^*, of the exponential strain energy function fits shown in Figure 4. Discrepancies between the values are most likely due to the approximation of l_0. Additionally, our method of approximating λ_{max} assumes that all midblock strands will be fully extended before breakdown of the network. In reality, the physical cross-links of the network will not be able to withstand the necessary stress for molecular reorganization into a fully extended *trans*-conformation.

The similarity between γ_{max} and γ^* is consistent with our hypothesis that the value of the critical strain, γ^*, at which stress-divergence occurs due to strain stiffening is controlled by the finite extensibility, and ultimately the overall length, of the midblock. The hydrogel samples also displayed mechanical behavior consistent with these results (see Figure 6), although we do not have comparable scattering data for these polymers from which l_0 can be determined. However, relative magnitudes of J^* were consistent with the relative midblock length, with the network having the larger value of l_{max} also having the larger value for γ^*.

Thus far, we have shown that by varying the length of network strands (i.e., midblock length), the onset of nonlinear strain stiffening is tunable. Connections can be made to fibrous biopolymer networks of actin cross-linked with various actin-binding proteins (ABPs). The strain-stiffening behavior of these actin-based networks is dominated by the properties of the cross-linking molecules rather than by the actin filaments.[44] Wagner and co-workers[45] demonstrated that small changes in the structure of the cross-linking molecule greatly affect the nonlinear mechanical response of actin networks. Specifically, the onset of strain stiffening increases to larger values of strain as the length of the cross-linker increases. Figure 7 shows the shear deformation behavior of actin networks cross-linked by ABPs of different lengths. As seen in the figure, strain stiffening of the network cross-linked by the shorter molecule becomes dominant at a smaller value of strain than the strain stiffening of the network cross-linked by the longer molecule.

Table 2. Predicted Maximum Strain and Observed Critical Strain for Physically Associating Networks of ABA and ACA Triblock Copolymers

polymer	Φ_p	J^*	D (nm)	l_0 (nm)	l_{max} (nm)	λ_{max}	γ_{max}	γ^*
$A_{25}B_{116}A_{25}$	0.035	17	50	40	231	5.8	5.6	4.1
$A_9B_{53}A_9$	0.05	14	38	28	106	3.8	3.5	3.7
$A_{23}B_{31}A_{23}$	0.07	3.5	34	24	61	2.5	2.1	1.9
$A_{22}C_{45}A_{22}$	0.10	7			134			2.6
$A_{34}C_{114}A_{34}$	0.10	35			339			5.9

The exponential strain energy function used to capture the strain-stiffening behavior of our synthetic networks also captures the stress response of the cross-linked actin networks and is represented by the solid lines in Figure 7. Stiffening becomes significant at a larger value of strain for the network containing the longer cross-linking molecule, consistent with the notion that the strain-stiffening behavior of both the cross-linked actin networks and the synthetic physically associating networks is controlled by the length and subsequent stretching of a compliant network strand.[45] Interestingly, as described in the Introduction, the exponential constitutive model also describes the strain-stiffening behavior of semiflexible fibrous networks of other biopolymers such as collagen, fibrin, and vimentin, even though many of these networks stiffen at much lower strains than our synthetic networks.[1] As reported in Table 3 and illustrated in Figure 1 with data taken from Storm et al.,[1] a number of different biopolymer networks exhibit behavior that is accurately described by the exponential strain-stiffening model. This

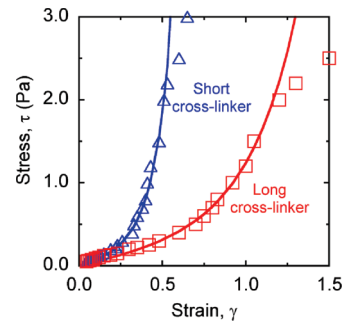

Figure 7. Strain-stiffening behavior during steady shear deformation ($\dot{\gamma} = 0.125\ s^{-1}$) of two fibrous actin networks cross-linked by actin-binding proteins of different lengths. (Data taken from Wagner et al.[45]) Solid lines represent eq 4 for the short cross-linker data (HisAc-D2-6, 125 kDa; $G_0 = 0.7$ Pa and $J^* = 0.15$) and long cross-linker data (ddFLN, 250 kDa; $G_0 = 0.5$ Pa and $J^* = 1.1$).

Table 3. Estimated Exponential Strain Energy Function Parameters and Resulting Critical Strains for some Common Biomaterials

material	G_0 (Pa)	J^*	γ^*
collagen[a]	13	0.010	0.10
actin[a]	90	0.015	0.12
vimentin[a]	3.7	0.13	0.36
actin, short cross-link[b]	0.7	0.15	0.39
fibrin[a]	18	0.15	0.39
actin, long cross-link[b]	0.5	1.1	1.0
$A_{23}B_{31}A_{23}$; $\phi_p = 0.07$	1200	3.5	1.9
neurofilaments[a]	2.3	9	3
$A_9B_{53}A_9$; $\phi_p = 0.05$	400	14	3.7
$A_{25}B_{116}A_{25}$; $\phi_p = 0.035$	350	17	4.1

[a] Storm et al.[1] [b] Wagner et al.[45]

similarity of behavior does not confirm a common physical structure or stiffening mechanism between biopolymer networks and our synthetic physically associating networks. In fact, the underlying network structure (e.g., levels of entanglement, strand flexibility) is expected to be quite different. For example, the mixture of entropic and enthalpic (i.e., bending) elasticity that is believed to drive the strain-stiffening response of semiflexible biopolymer networks is in contrast to the purely entropic elasticity which is dominant in many physically associating networks.[1,3,46,47] However, the similar phenomenology of the strain-stiffening behavior indicates that our synthetic physically associating networks can be excellent model systems for biological materials in the nonlinear regime since (1) the nonlinear responses of both the biopolymer and the physically associating networks can be quantified by an exponential strain energy function with J^* values related to the structure of the networks and (2) the structure of the physically associating networks can be manipulated during synthesis to yield the nonlinear response that is representative of some actual biopolymer networks.

Conclusions

The strain-stiffening behavior of model elastic networks of physically associating polymers has been characterized by shear rheometry. Our results demonstrate a clear correlation between network structure, specifically, variation in midblock length, and strain-stiffening behavior. The observed stiffening response is accurately captured by an exponential strain energy function with a single fitting parameter in addition to the small-strain modulus. For our model networks based on triblock copolymer solutions, this parameter depends primarily on the molecular weight of the midblock. This same constitutive model can be used to describe a variety of biopolymer networks, even though the mechanisms of elasticity may be fundamentally different. The similarity in the phenomenological behavior of these different types of gels has two important implications. First, our stiffening model provides a way of characterizing the nonlinear mechanical response using a single parameter that we have tabulated for a variety of disparate biopolymer networks. The second implication of the similarity between the biological and the synthetic networks is that the synthetic networks could be used to create biomaterials with the desired stiffening properties or as model synthetic systems with tunable behavior for use in future studies of nonlinear elasticity and fracture in biological materials.

Acknowledgment. This work was supported through the National Science Foundation through Grant CMMI-0900586. An NSF fellowship to K.A.E. is also acknowledged, as is the use of facilities provided by the Northwestern University Materials Research Center through the NSF MRSEC program (DMR-0520513).

References and Notes

(1) Storm, C.; Pastore, J. J.; MacKintosh, F. C.; Lubensky, T. C.; Janmey, P. A. *Nature* **2005**, *435* (7039), 191–194.
(2) Janmey, P. A.; Winer, J. P.; Weisel, J. W. *J. R. Soc. Interface* **2009**, *6* (30), 1–10.
(3) Gardel, M. L.; Shin, J. H.; MacKintosh, F. C.; Mahadevan, L.; Matsudaira, P.; Weitz, D. A. *Science* **2004**, *304* (5675), 1301–1305.
(4) Pollard, T. D.; Cooper, J. A. *Science* **2009**, *326* (5957), 1208–1212.
(5) Kandow, C. E.; Georges, P. C.; Janmey, P. A.; Beningo, K. A. Polyacrylamidc hydrogels for cell mechanics: Steps toward optimization and alternative uses. *Cell Mechanics*; Elsevier Academic Press, Inc.: San Diego, 2007; Vol. 83, p 29.
(6) Treloar, L. R. G. *The physics of rubber elasticity*, 3rd ed.; Clarendon Press: Oxford, 1975.
(7) Pellens, L.; Corrales, R. G.; Mewis, J. *J. Rheol.* **2004**, *48* (2), 379–393.
(8) Berret, J. F.; Séréro, Y.; Winkelman, B.; Calvet, D.; Collet, A.; Viguier, M. *J. Rheol.* **2001**, *45* (2), 477–492.
(9) Seitz, M. E.; Martina, D.; Baumberger, T.; Krishnan, V. R.; Hui, C. Y.; Shull, K. R. *Soft Matter* **2009**, *5* (2), 447–456.
(10) Séréro, Y.; Aznar, R.; Porte, G.; Berret, J. F.; Calvet, D.; Collet, A.; Viguier, M. *Phys. Rev. Lett.* **1998**, *81* (25), 5584–5587.
(11) Noro, A.; Matsushita, Y.; Lodge, T. P. *Macromolecules* **2008**, *41* (15), 5839–5844.
(12) Drzal, P. L.; Shull, K. R. *Macromolecules* **2003**, *36* (6), 2000–2008.
(13) Kumar, S. K.; Douglas, J. F. *Phys. Rev. Lett.* **2001**, *87* (18), 4.
(14) Tanaka, F. *Polym. J.* **2002**, *34* (7), 479–509.
(15) Vermonden, T.; Besseling, N. A. M.; van Steenbergen, M. J.; Hennink, W. E. *Langmuir* **2006**, *22* (24), 10180–10184.
(16) Liu, R. X.; Fraylich, M.; Saunders, B. R. *Colloid Polym. Sci.* **2009**, *287* (6), 627–643.
(17) Liu, W. G.; Zhang, B. Q.; Lu, W. W.; Li, X. W.; Zhu, D. W.; De Yao, K.; Wang, Q.; Zhao, C. R.; Wang, C. D. *Biomaterials* **2004**, *25* (15), 3005–3012.
(18) Montgomery, J. K.; Drzal, P. L.; Shull, K. R.; Faber, K. T. *J. Am. Ceram. Soc.* **2002**, *85* (5), 1164–1168.
(19) Erk, K. A.; Dunand, D. C.; Shull, K. R. *Acta Mater.* **2008**, *56* (18), 5147–5157.
(20) Chang, D. P.; Dolbow, J. E.; Zauscher, S. *Langmuir* **2007**, *23* (1), 250–257.
(21) Cordier, P.; Tournilhac, F.; Soulie-Ziakovic, C.; Leibler, L. *Nature* **2008**, *451* (7181), 977–980.
(22) Werten, M. W. T.; Teles, H.; Moers, A.; Wolbert, E. J. H.; Sprakel, J.; Eggink, G.; de Wolf, F. A. *Biomacromolecules* **2009**, *10* (5), 1106–1113.
(23) Wang, Y. C.; Tang, L. Y.; Li, Y.; Wang, J. *Biomacromolecules* **2009**, *10* (1), 66–73.
(24) Pratoomsoot, C.; Tanioka, H.; Hori, K.; Kawasaki, S.; Kinoshita, S.; Tighe, P. J.; Dua, H.; Shakesheff, K. M.; Rose, F. *Biomaterials* **2008**, *29* (3), 272–281.
(25) He, C. L.; Kim, S. W.; Lee, D. S. *J. Controlled Release* **2008**, *127* (3), 189–207.
(26) Mowery, C. L.; Crosby, A. J.; Ahn, D.; Shull, K. R. *Langmuir* **1997**, *13* (23), 6101–6107.
(27) Seitz, M. E.; Burghardt, W. R.; Faber, K. T.; Shull, K. R. *Macromolecules* **2007**, *40* (4), 1218–1226.
(28) Bras, R. E.; Shull, K. R. *Macromolecules* **2009**, *42* (21), 8513–8520.
(29) Schoch, A. B.; Henderson, K. J.; Brinson, L. C.; Shull, K. R. 2010, manuscript in preparation.
(30) Guvendiren, M.; Shull, K. R. *Soft Matter* **2007**, *3* (5), 619–626.
(31) Zhou, J.; Fung, Y. C. *Proc. Natl. Acad. Sci. U.S.A.* **1997**, *94* (26), 14255–14260.
(32) Douglas, J. F. *Mater. Res. Soc. Symp. Proc.* **2010**, *1234*, 1234-QQ04-01.
(33) Berret, J. F.; Séréro, Y. *Phys. Rev. Lett.* **2001**, *87* (4), 048303.
(34) Baumberger, T.; Caroli, C.; Martina, D. *Nat. Mater.* **2006**, *5* (7), 552–555.
(35) Rubinstein, M.; Panyukov, S. *Macromolecules* **2002**, *35* (17), 6670–6686.
(36) Colby, R. H.; Rubinstein, M. *Macromolecules* **1990**, *23* (10), 2753–2757.
(37) Milner, S. T. *Macromolecules* **2005**, *38* (11), 4929–4939.
(38) Creton, C.; Hu, G. J.; Deplace, F.; Morgret, L.; Shull, K. R. *Macromolecules* **2009**, *42* (20), 7605–7615.
(39) Séréro, Y.; Jacobsen, V.; Berret, J. F.; May, R. *Macromolecules* **2000**, *33* (5), 1841–1847.
(40) Tung, S. H.; Raghavan, S. R. *Langmuir* **2008**, *24* (16), 8405–8408.
(41) Tam, K. C.; Jenkins, R. D.; Winnik, M. A.; Bassett, D. R. *Macromolecules* **1998**, *31* (13), 4149–4159.
(42) Rubinstein, M.; Colby, R. H. *Polymer Physics*; Oxford University Press: Oxford; New York, 2003; Vol. xi, p 440.
(43) Percus, J. K.; Yevick, G. J. *Phys. Rev.* **1958**, *110* (1), 1–13.
(44) Gardel, M. L.; Nakamura, F.; Hartwig, J.; Crocker, J. C.; Stossel, T. P.; Weitz, D. A. *Phys. Rev. Lett.* **2006**, *96* (8), 4.
(45) Wagner, B.; Tharmann, R.; Haase, I.; Fischer, M.; Bausch, A. R. *Proc. Natl. Acad. Sci. U.S.A.* **2006**, *103* (38), 13974–13978.
(46) Chaudhuri, O.; Parekh, S. H.; Fletcher, D. A. *Nature* **2007**, *445* (7125), 295–298.
(47) Onck, P. R.; Koeman, T.; van Dillen, T.; van der Giessen, E. *Phys. Rev. Lett.* **2005**, *95* (17), 4.

BM100136Y